IEEE Access
Multidisciplinary | Rapid Review | Open Access Journal

Received 26 September 2022, accepted 6 November 2022, date of publication 14 November 2022,
date of current version 17 November 2022.

Digital Object Identifier 10.1109/ACCESS.2022.3221747

RESEARCH ARTICLE

Optimization of a Color-Based Spatial Modulation Scheme for VLC Under Illuminance and SINR Constraints

GALEFANG A. MAPUNDA[1,2], ABRAHAM SANENGA[1,2], BOKAMOSO BASUTLI[1], (Senior Member, IEEE), AND JOSEPH M. CHUMA[1], (Member, IEEE)

[1]Signal Processing, Networks and Systems Research Group, Department of Electrical, Computer and Telecommunication Engineering, Botswana International University of Science and Technology, Palapye, Botswana
[2]National Astronomical Research Institute of Thailand, Chiang Mai 50180, Thailand

Corresponding author: Galefang A. Mapunda (galefang.mapunda@studentmail.biust.ac.bw)

This work was supported by the Botswana International University of Science and Technology (BIUST) under Initiation Research Grant S00077.

ABSTRACT This treatise presents a framework for the optimisation of a colour-based optical spatial modulation for visible light communication (VLC). The focus is particularly on the conflicting interests between illuminance and signal transmission. The system under consideration is configured with a non-line-of-sight (NLoS) model, based on the joint use of colour shift keying (CSK) and optical spatial modulation (OSM) with intensity modulation and direct detection (IM/DD). With the adaptation of the aforementioned optical techniques and convex optimisation, the design and development of a colour-based optical wireless system is carried out. Firstly, an optimisation problem with the intention of minimising the total luminous intensities of the light emitting diode (LED) arrays subject to the transmitting LED array's optical power budget, minimum required illuminance level, LED-user channel conditions and latency intolerant users' (LITUs) quality-of-service (QoS) target constraints is defined. Secondly, a coordinated algorithm for the selection of a transmitting LED array, maintenance of a particular illuminance and signal-to-interference-plus noise ratio (SINR) levels during symbol transmission is designed. Lastly, through computer simulations, a numerical analysis is carried out to demonstrate and evaluate the performance of the algorithm. During the transmission of all symbols, the proposed framework is capable of satisfying the SINR target for LITUs while reducing the optical power by approximately 20% to 25% and 20% to 75% for transmitting and non-transmitting LED arrays, respectively. Additionally, provided that the required illuminance level is specified within the standardised levels of 300 lux to 1500 lux, the proposed system can provide adequate illuminance as per the users' requirement at all points where either a LITU or a latency tolerant user (LTU) is located at any given instance. However, fair SINR levels are not guaranteed at the points where the LTUs are positioned. On the other hand, the algorithm disposes low illuminance levels ranging from 100 lux to 250 lux at locations towards the room boundaries where there are no users. The proposed system is able to achieve data rates of 5 Mbps to 25 Mbps using commercially-off-the-shelf LEDs.

INDEX TERMS Colour, illumination, line-of-sight, optimisation, visible light communication, wireless.

I. INTRODUCTION

Illumination is on the verge of being completely restructured because of the advancements in the solid-state lighting (SSL) domain. Contemporary incandescent and fluorescent lamps are rapidly being replaced by SSL luminaires, which have higher energy efficiency, higher brightness and light uniformity [1]. SSL luminaires, in particular, light emitting diode (LED) and laser diode (LD) luminaires are desirable for their capability to switch between different levels of

The associate editor coordinating the review of this manuscript and approving it for publication was Christos Anagnostopoulos.

luminous intensity at an extremely high rate, which enables SSL luminaires to also be used for visible light communication (VLC) [2], [3]. In VLC, spatial arrays consisting of a single or multi-colour light sources are typically employed for a dual purpose, being the provision of illumination and data transmission over a wireless channel. Conventionally, LEDs are widely used instead of LDs for the establishment of VLC systems due to their smaller footprint, ease of installation, wider output beam pattern, lower cost, longer life-span and lower heat dissipation. The limited use of LDs is driven by the possible health hazard concerns as well as colour mixing complexity [4]. Owing to the dual purpose of the lighting sources in VLC, it is substantial to come up with efficient techniques for resource allocation to mitigate the negative impacts of the conflicting interests between illuminance and data transmission.

Multiple-input multiple-output (MIMO) systems have been widely studied for implementation in optical wireless communication (OWC) systems, particularly VLC. Optical spatial modulation (OSM), is one of the MIMO algorithms utilised for the facilitation of data transmission for indoor VLC systems. OSM is conceptualised based on the idea of spatial modulation (SM). Therefore, OSM is inherently capable of attaining higher spectral efficiency. Besides, OSM is completely robust to inter-channel interference (ICI) and this property simplifies symbol decoding on the receiver unit [5]. With that being said, OSM based systems can result in a sub-optimal performance due to two main shortfalls. The first being, OSM does not simultaneously use all of the available LED or LD lamps as transmitters for data transmission, which leads to reduced data rates when compared to other MIMO techniques. Lastly, when a channel is highly correlated, as is the case when using non-imaging receivers, there is a significant power loss [6].

As a means of augmenting the overall performance of OSM-based systems, other techniques can be appropriately used synchronously with OSM. The standardised IEEE 802.15.7 colour shift keying (CSK) modulation in [7] is one of those techniques that possess advantageous qualities to be integrated with OSM. In CSK, the signal constellation points are defined based on the mixture of three different colour bands (red, green and blue) of the multi-coloured light source. CSK technique is one of the favourable VLC modulation techniques due to its ability to offer higher data transmission speeds [7]. Multi-colour sources on their own intrinsically form a colour space MIMO, which can lead to elevated data throughput [8], [9]. Different CSK constellation sizes may be used depending on the data rate requirement. Moreover, there are no known negative impacts to the human vision on account of the constant power of the modulated signals, resulting in flicker-free illumination. On the other hand, due to the restricted freedom of the constellation symbols, the optimised minimum Euclidean distance of CSK symbols is much smaller compared to techniques such as quadrature amplitude modulation. Symbol restriction emanates from the colour space chromaticity diagram shown in Figure 1 as

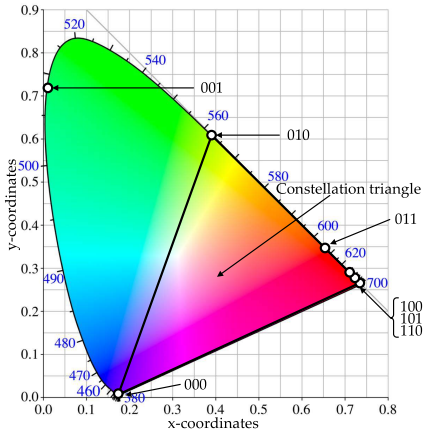

FIGURE 1. CIE 1931 colour space chromaticity diagram.

defined by the International Commission on Illumination 1931 (CIE 1931) [10]. This diagram confines the CSK constellation symbols to only a portion of its shape.

Various studies on OSM and CSK techniques have been widely carried out. For the relevant background on OSM and CSK, the reader is referred to some of the recent research works in [11], [12], [6], and [13] on OSM whereas part of the recent literature on CSK is presented in [7], [14], [15], and [16].

Joint utilisation of OSM and CSK is capable of meeting particular data rate specifications with low-order system complexity. On the other hand, the integration of the two techniques yield an improved system performance as it reaps the benefits of elevated data rates from the colour domain of CSK and the spatial gain from the spatial domain of OSM [8]. In the proposed system, concurrent exploitation of both OSM and CSK for adequate room illumination as well as data transmission with priority given to latency intolerant users (LITUs) is considered. To the best of the authors' knowledge, at the time of writing this paper, there has only been two papers [8], [9], which focused on the joint use of CSK and OSM for MIMO systems in VLC. However, the authors of the existing works in [8] and [9] did not consider the omnipresence of heterogeneous users of the network. Moreover, the authors did not look into the provision of adequate illuminance at different points of the room during data transmission.

Unlike the works in [8] and [9], this study considers the optimisation of a multi-user system under various constraints in a heterogeneous user network (i.e users have different quality-of-service (QoS) requirements). The proposed system is configured as an indoor non-line-of-sight (NLoS) model based on the collaborative use CSK and OSM with IM/DD. The considered system model for this work is adapted from [8] but with the capability of transmitter re-assignment based on the location of the user that is being served. This allows efficient provision of the desirable QoS to all LITUs. The proposed scheme is also capable of allocating adequate illuminance at all points where users are located. To the extent

of the authors' knowledge, the authors believe that it is the first time that the consideration of power minimisation in the presence for heterogeneous users is being investigated for application in VLC systems. In addition, the simulation results presented in this paper have not been previously reported in the literature.

The remaining part of this article is structured as follows. In Section II, the functional units of the proposed scheme are presented. Section III provides the optimisation model of the proposed system. In Section IV, simulation results are provided to demonstrate the performance of the algorithm. Lastly, in Section V, the study is concluded based on the technical findings of the previous sections. Furthermore, in the same section, the pros and cons of the proposed system as well as some of the future works are discussed.

II. FUNCTIONAL MODEL

Joint utilisation of CSK and OSM is capable of meeting data rate specifications with low-order complexity. On the other hand, the integration of the two techniques yield an improved system performance as it reaps the benefits of elevated data rates from the colour domain and the spatial gain from the spatial domain [8], [9]. For avoidance of ambiguity and confusion, uppercase and boldface font is used to represent matrices while vectors are represented by lowercase and boldface font.

A. SIGNAL MODULATION

The core block diagram of the proposed scheme based on CSK is shown in Figure 2. Let $\mathbf{X}$ denote the input binary data carrying matrix block. This input block is defined by $N_b \times \mathcal{N}$, where, $\mathcal{N}$ represents the total number of symbols in a colour-based OSM whereas N_b is the total number of bits transmitted per symbol and it is defined by [8]

$$N_b = \log_2 M + \log_2 N_T, \tag{1}$$

where M is the constellation size and N_T is the total number of optical transmitter arrays. The vectors of $\mathbf{X}$, given by $\left[\mathbf{x}_0, \mathbf{x}_1, \ldots, \mathbf{x}_{\mathcal{N}-1}\right]^{\mathsf{T}}$ are individually mapped to the available LED arrays and also to the different constellation points in the colour (signal) domain. Data symbols have two variables of bits, which are the most significant bits (MSBs) and the least significant bits (LSBs). The MSBs of the data symbol are mapped to CSK constellation points in the colour domain while the LSBs are mapped to the indices of the LED arrays. The mapping facilitates the selection and activation of the transmitting LED array in the spatial domain according to the pre-defined mapping table. The activated array will in-turn simultaneously illuminate the room and transmit data to all users. Like the colour domain, the spatial domain is also carrying data. An illustration of the mapping procedure of the colour-based OSM using 8-CSK and four LED transmitter arrays is shown in Figure 2. During the mapping process, $\mathbf{X}$ is transformed into a new chromaticity mapping matrix $\mathbf{Z}$, defined by $(N_T \times 2) \cdot \mathcal{N}$. Subsequently, $\mathbf{Z}$ is transformed into an intensity matrix $\mathbf{U}$ with dimensions $(N_T \times 3) \cdot \mathcal{N}$ [8].

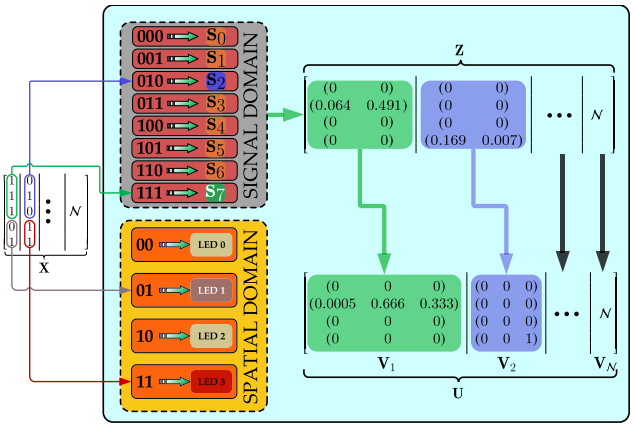

FIGURE 2. Colour-based OSM mapping procedure using 8-CSK and four LEDs. Adapted from [8].

To delineate the mapping process, consider the first symbol $\mathbf{x}_0 = [1\ 1\ 1\ 0\ 1]^{\mathsf{T}}$ as depicted in Figure 2. The MSBs (first three bits) of this transmission symbol are mapped to one of the points in the 8-CSK signal domain, which in this case is expressed by $\mathbf{s}_7$. CSK constellation points are determined based on their xy-chromaticity coordinates as defined in [7] with reference to the CIE 1931 chromaticity diagram shown in Figure 1. The LSBs (last two bits) are used to select and activate one of the LED transmitter arrays, which in this case is LED array denoted as LED 1. The same procedure is then followed for the next symbol $[0\ 1\ 0\ 1\ 1]^{\mathsf{T}}$ until all $\mathcal{N}$ symbols have been transmitted [12].

Upon completion of the $\mathbf{X}$ conversion, the non-zero xy-chromaticity coordinates contained in the column vectors of the sub-matrices in $\mathbf{Z}$ can now be converted into their weighted x and y luminous intensity (chromaticity) values. This conversion is facilitated by Figure 1 and solving a system of linear equations given by

$$\begin{cases} s_i x_i + s_j x_j + s_k x_k = x \\ s_i y_i + s_j y_j + s_k y_k = y \\ s_i + s_j + s_k = 1, \end{cases} \tag{2}$$

where, s_i, s_j and s_k are the CSK symbol intensities, with a symbol defined as, $\mathbf{s} = \left[s_i, s_j, s_k\right]$. As shown in Figure 2, all rows of the sub-matrices in $\mathbf{U}$ have only one non-zero row and this row corresponds with the LED number that is activated during symbol transmission. Detailed guidelines of CSK modulation are given by the IEEE 802.15.7 standard in [7]. The modulated intensities are then used to control the light emission of the transmitter following the same concept of OSM as defined in [12].

B. OPTICAL CHANNEL

An optical channel is mainly characterised by the DC channel gain between the transmitter and receiver as defined by [17] where, $A_r, m_1, \phi, T_s, g, \psi, d$ are respectively, active collection area, LED's Lambertian order, irradiance angle, optical filter's gain, optical concentrator gain, incidence angle, distance

between the receiver and the transmitter and finally, ψ_c is the optical detector's field-of-view (FOV). Equation 3, as shown at the bottom of the page, only considers the line-of-sight (LoS) components, however, various aspects such as, but not limited to; surface material, the angle of incidence and roughness of the surface (e.g walls and ceiling) relative to the transmission wavelength (i.e wavelength-dependent reflectance of surfaces) as well as the orientation and positioning of the transmitter-receiver pair must be considered for a robust and reliable channel gain. A consideration of the aforementioned aspects (which defines the reflected path's channel gain) together with the LoS DC channel gain yield [17]

$$h_{NLoS} = h_{LoS}(0) + \sum_{i=1}^{REFL} h_i(0), \tag{4}$$

where *REFL* is the number of reflecting elements and $h_i(0)$ is the NLoS channel gain from the path of the reflecting object/surface defined in (5), as shown at the bottom of the next page, where ρ_i represents the reflection coefficient of reflector i, dA represents the reflective area of the reflecting region, ϕ_{1i} is the transmission angle between the transmitter/source and reflector i, α_i is the angle of incidence on the reflecting surface, β_i is the angle of irradiance from the reflector to the receiver. The distance between the transmitter-reflector pair and the reflector-receiver pair are represented by d_{1i} and d_{2i}, respectively. The considered model for this work is graphically depicted in Figure 3. The total instantaneous optical power at the receiver is expressed as

$$\mathbf{p}_r = \mathbf{H}\mathbf{p}_l^{\max}, \tag{6}$$

where, $\mathbf{p}_l^{\max}$ is the maximum transmitting optical power. $\mathbf{H}$ is a $N_R \times N_T$ channel gain matrix, with N_R being the total number of receivers. The individual entries of $\mathbf{H}$ define the channel gains between the pairs of the multi-luminaire LEDs chip and the PD. For instance, the $(N_T \times 3)$-dimensional vector, $\mathbf{h}_{ij}$ is the channel gain vector between the RGB transmitter i and the RGB receiver j, i.e, $\mathbf{h}_{ij} = [h_{ij}^{(0)}, \cdots, h_{ij}^{(2)}]$.

C. RECEIVER

During one time interval T, of a colour-based OSM data symbol, one sub-matrix of $\mathbf{U}$ i.e. $\mathbf{V}_k$, is transmitted through a channel with N_T transmitters until all $\mathcal{N}$ symbols are transmitted. All transmitters have an array of RGB LED chips. The k-th received signal $\mathbf{r}_k$ at each receiver is expressed by

$$\mathbf{r}_k = \mathcal{R}\mathbf{h}_{ij}^{\mathsf{T}}\mathbf{V}_k + \mathbf{n}_k, \tag{7}$$

where $\mathbf{n}_k$ is the AWGN vector at the receiver. The noise vector has a variance of σ^2 and contains three independent

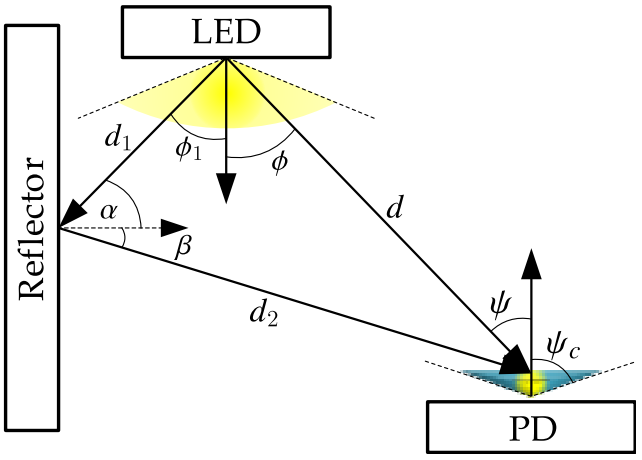

FIGURE 3. NLoS link configuration.

and identically distributed (i.i.d) elements with mean value of 0 and a noise variance of $\sigma_0^2 = \sigma^2/3$. At each detector, the variance σ_0^2 of the AWGN is modelled as a summation of the shot noise and thermal noise, which are respectively defined by [18]

$$\sigma_Q^2 = 2q_e\langle i\rangle B, \tag{8a}$$

$$\sigma_{TH}^2 = \frac{4k_B T_k B}{R_L}, \tag{8b}$$

where, q_e is the electronic charge, $\langle i\rangle$ is the average current over an instance of time, B is the bandwidth (in Hz) of the filter that follows the PD, k_B is the Boltzmann constant, T_k the absolute temperature (in K) and R_L is the load resistance. Therefore the SNR may be expressed as

$$\gamma_0 = \frac{\mathbb{E}\left\{\|\mathcal{R}\mathbf{p}_k\|^2\right\}}{\sigma_0^2}, \tag{9}$$

where $\mathbb{E}\{\cdot\}$ is the operation for the expected value defining the average received power, $\mathcal{R}$ is the responsivity of the optical detector and $\mathbf{p}_k$ is the received power of all legitimate colour domain symbols.

D. SIGNAL DEMODULATION

Due to the concurrent use of CSK and OSM modulation techniques, there is a need for joint demodulation of the CSK and OSM modulated symbols. The concatenated demodulation technique [8] or alternatively the joint maximum-likelihood (ML) based demodulation [19] are the two methods that could be used to demodulate the received signal. On account of improved performance and the ability to achieve demodulation of the colour-based OSM modulated symbols with a single attempt, joint ML-based demodulation is considered. With this technique, as opposed to its counterpart, both the transmitter index and CSK signal points are detected at once.

$$h_{LoS}(0) = \begin{cases} \dfrac{A_r(m_1+1)\cos^{m_1}(\phi)\,T_s(\psi)\,g(\psi)\cos(\psi)}{2\pi d^2}, & 0 \le \psi \le \psi_c \\ 0, & \psi \ge \psi_c, \end{cases} \tag{3}$$

In order to demodulate the CSK-modulated signals, each receiver must constitute three PDs with each having narrow-band optical colour filters of red, green and blue among other components.

A simple estimate of symbol $\mathbf{x}_k$, defined by $\hat{\mathbf{x}}_k$ can be done by the use of colour calibration to compensate for any impairments induced during signal propagation and the estimated symbol is defined by [7]

$$\hat{\mathbf{x}}_k = \mathcal{R}\mathbf{H}^{-1}\mathbf{r}_k. \tag{10}$$

In the event that $\mathbf{H}$ does not have a full rank, matrix inversion is infeasible. Under such a circumstance, the pseudo inverse of $\mathbf{H}$ can be used. On the other hand, detection techniques such as the maximum likelihood-aided detectors and lattice-reduction-aided detectors may be used. In this work, an estimate of $\mathbf{x}_k$, is obtained by means of determining the *a posteriori* probability of each symbol $\mathbf{x}_{\mathtt{t},\mathtt{c}}$, $\mathbf{x}_{\mathtt{t},\mathtt{c}} \in \mathbf{X}$. Symbol $\mathbf{x}_{\mathtt{t},\mathtt{c}}$ is expressed by

$$\mathbf{x}_{\mathtt{t},\mathtt{c}} = \mathcal{R}\mathbf{H}\mathbf{V}_{\mathtt{t},\mathtt{c}}, \tag{11}$$

where $\mathbf{V}_{\mathtt{t},\mathtt{c}}$ is a $N_T \times 3$ matrix. The $\mathtt{t}$-th row of matrix $\mathbf{V}_{\mathtt{t},\mathtt{c}}$ contains the light weighted intensities $(s_i,\ s_j$ and $s_k)$ of the RGB LED chips while all other rows of the matrix contains values of zero signifying that there is only one specific transmitter activated during the transmission time interval of one symbol. The intensities of the RGB LED chips are obtained from the $\mathtt{c}$-th point of the M-ary CSK constellation point. Hence the *a posteriori* probability is denoted by [20], [19], and [8]

$$\begin{aligned}\Pr\left(\mathbf{x}_{\mathtt{t},\mathtt{c}}|\mathbf{r}_k\right) &= \mathrm{p}\left(\mathbf{r}_k|\mathbf{x}_{\mathtt{t},\mathtt{c}}\right)\frac{\Pr\left(\mathbf{x}_{\mathtt{t},\mathtt{c}}\right)}{\mathrm{p}\left(\mathbf{r}_k\right)} \\ &= \frac{\Pr\left(\mathbf{x}_{\mathtt{t},\mathtt{c}}\right)}{2\pi\sigma\,\mathrm{p}\left(\mathbf{r}_k\right)}\exp\left(\frac{-\left\|\mathbf{r}_k - \mathbf{x}_{\mathtt{t},\mathtt{c}}\right\|^2}{2\sigma^2}\right),\end{aligned} \tag{12}$$

where $\Pr\left(\mathbf{x}_{\mathtt{t},\mathtt{c}}\right)$ is the a priori probability of symbol $\mathbf{x}_{\mathtt{t},\mathtt{c}}$. In the log domain, Equation 12 may be represented as

$$\mathrm{lr}\left(\mathbf{x}_{\mathtt{t},\mathtt{c}}|\mathbf{r}_k\right) = A - \left(\frac{\left\|\mathbf{r}_k - \mathbf{x}_{\mathtt{t},\mathtt{c}}\right\|^2}{2\sigma^2}\right), \tag{13}$$

where $A = \ln\left[\Pr\left(\mathbf{x}_{\mathtt{t},\mathtt{c}}\right)\right] - \ln\left[2\pi\sigma\,\mathrm{p}\left(\mathbf{r}_k\right)\right]$. In the absence of priori information, A is the same for all symbols and $\mathrm{lr}\left(\mathbf{x}_{\mathtt{t},\mathtt{c}}|\mathbf{r}_k\right)$ is defined by $\ln\left[\Pr\left(\mathbf{x}_{\mathtt{t},\mathtt{c}}|\mathbf{r}_k\right)\right]$. Therefore, Equation 13 is used to estimate Symbol $\mathbf{x}_{\mathtt{t},\mathtt{c}}$ as the ML function and the maximum a posteriori probability (MAP) estimate is defined by [20], [19], and [8]

$$\hat{\mathbf{x}}_k = \{\hat{\mathtt{t}}, \hat{\mathtt{c}}\} = \arg\max_{\mathtt{t},\mathtt{c}}\left[\mathrm{lr}\left(\mathbf{x}_{\mathtt{t},\mathtt{c}}|\mathbf{r}_k\right)\right]$$

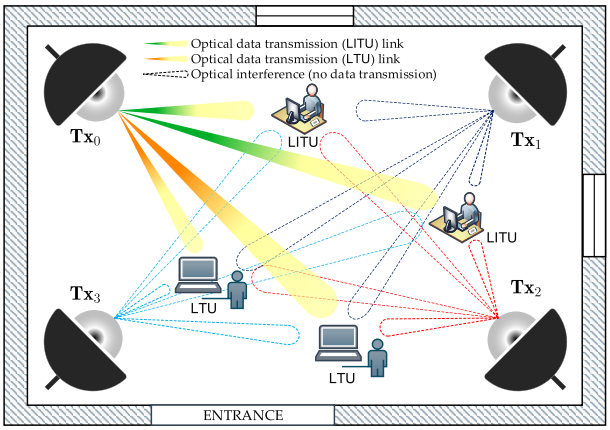

FIGURE 4. Colour-based OSM network with LITUs and LTUs.

$$= \arg\min_{\mathtt{t},\mathtt{c}}\left\|\mathbf{r}_k - \mathbf{x}_{\mathtt{t},\mathtt{c}}\right\|^2. \tag{14}$$

The symbol $\mathbf{x}_{\mathtt{t},\mathtt{c}}$, with the least distance from the received symbol $\mathbf{r}_k$, can now be regarded as the legitimate symbol $\hat{\mathbf{x}}_k$. The demodulated index of the LED is expressed as $\hat{\mathtt{t}}$ and the constellation point is denoted by $\hat{\mathtt{c}}$ [8]. Subsequently, there is conversion of the constellation point back to the *xy*-chromaticity coordinates and finally the decoding module is used to retrieve the bit stream of symbol $\mathbf{x}_k$.

III. OPTIMIZATION MODEL

Consider a typical multicast and coordinated downlink indoor VLC system configured with a NLoS model with L transmitters, G groups of users and U users. All transmitters have an array of RGB LED chips. The sets of transmitters, groups and users are denoted by $\mathcal{L} = \{1, \ldots, L\}$, $\mathcal{G} = \{1, \ldots, G\}$, and $\mathcal{U} = \{1, \ldots, U\}$, respectively. As depicted in Figure 4, at any given instance of a data symbol transmission, only one of the L transmitters (as shown with colour filled solid lines) is selected and activated for data transmission as well as illumination while the other transmitters (as shown with unfilled dashed lines) are strictly activated for augmenting illumination.

The number of groups which are served by transmitter l is defined as G_l, where the corresponding set of groups is given by $\mathcal{G}_l$. The number of users in group g is represented by U_g and the corresponding set of users is denoted by $\mathcal{U}_g$. Each user can be a member of only one group, therefore, the sets of users who are members of different groups have no elements in common, meaning that they are disjoint and this is defined by $\mathcal{U}_a \cap \mathcal{U}_b = \varnothing, \forall_{a,b} \in \mathcal{G}, a \neq b$. Each of the optical transmitter arrays have maximum and equal transmission power of $p_l^{\max}$.

$$h_i(0) = \begin{cases} \dfrac{A_r \rho_i dA\,(m_1+1)\cos^{m_1}(\phi_{1i})\cos(\alpha_i)\cos(\beta_i)}{(2\pi d_{1i} d_{2i})^2}, & 0 \le \psi \le \psi_c \\ 0, & \psi \ge \psi_c, \end{cases} \tag{5}$$

Given a data symbol from the l-th transmitter to the u-th user, the transmitted signal, which is inferred to be non-negative for intensity modulation suitability, is given by [21]

$$\mathbf{x}_l = \frac{\tau \mathbf{V}_g}{\sqrt{T}}, \tag{15}$$

where τ is the optical source conversion factor for intensity modulation in W/A and $\mathbf{V}_g \in \mathbb{R}^{L\times 3}$ is the data symbol matrix. The signal received by user, u, is given by

$$y_u = \mathcal{R}\mathbf{h}_{l,u}^{\mathsf{T}}\mathbf{x}_l + \sum_{j\in\mathcal{L}\setminus\{l\}} \mathbf{h}_{j,u}^{\mathsf{T}}\mathbf{p}_j + \mathbf{n}_u, \quad \forall l \in \mathcal{L},\ \forall u \in \mathcal{U}_g \tag{16}$$

where $\mathbf{h}_{l,u}^{\mathsf{T}} \in \mathbb{R}^{1\times L}$ is the channel gain vector between the l-th transmitting LED array and the u-th user, $\mathbf{h}_{j,u}^{\mathsf{T}} \in \mathbb{R}^{1\times L}$ is the channel gain vector between the j-th non-transmitting LED array and the u-th user. The noise vector of the u-th user is denoted by $\mathbf{n}_u \in \mathcal{CN}\left(0, \sigma^2\right)$ and it has the same properties as defined for equation 7 [22]. The notation $\mathcal{L}\setminus\{l\}$ represents a set $\mathcal{L}$ excluding member l. It now follows that, the SINR of user u belonging to group g is defined by

$$\mathsf{SINR}_u = \frac{\left(\mathbf{h}_{l,u}^{\mathsf{T}}\mathbf{p}_l\right)^2}{\sum\limits_{j\in\mathcal{L}\setminus\{l\}}\left(\mathbf{h}_{j,u}^{\mathsf{T}}\mathbf{p}_j\right)^2 + \sigma_u^2}. \tag{17}$$

The horizontal illuminance on surface s, during symbol transmission is linearly dependent on the luminous intensities of the LED arrays [22], hence it is defined by

$$\mathcal{E}_{\mathsf{s}}^{\mathsf{tx}} = \underbrace{\frac{\mathcal{I}_{N_{l,u}}\cos^{m_1}(\phi)}{d_{l,u}^2\cos(\psi)}}_{\mathcal{E}_{\mathsf{TX}}} + \underbrace{\sum_{j\in\mathcal{L}\setminus\{l\}}\frac{\mathcal{I}_{N_{j,u}}\cos^{m_1}(\phi)}{d_{j,u}^2\cos(\psi)}}_{\mathcal{E}_{\mathsf{nTX}}}, \tag{18}$$

where $\mathcal{I}_{N_{l,u}}$ and $\mathcal{I}_{N_{j,u}}$ are the combined (i.e white) maximum luminous intensities of the transmitting array and non-transmitting arrays in the normal direction respectively. $d_{l,u}$ is the distance between the transmitting LED array and user u whereas $d_{j,u}$ is the distance between the non-transmitting LED array and user u. $\mathcal{E}_{\mathsf{TX}}$ and $\mathcal{E}_{\mathsf{nTX}}$ represents the illuminance of the transmitting and non-transmitting arrays respectively. Under the consideration of safety and visual efficiency, there is a minimum required illuminance, $\mathcal{E}_{\mathsf{r}_u}$, for every user station without any form of visual strain on the user at any given time instance.

The illuminance distribution across the working area must conform to a certain factor which is termed as illuminance uniformity. It is defined as the ratio of the lowest illuminance level to the average illuminance of uniformly distributed N sensors in the room [23]. It is therefore denoted as

$$\epsilon = \frac{\min\limits_{n}\left(\mathcal{E}_n\right)}{\frac{1}{N}\sum\limits_{n=1}^{N}\mathcal{E}_n} \tag{19}$$

A. ASSUMPTIONS

For this work, without any calculations or special considerations, a few assumptions were made as follows:

- for each receiver, there is an uplink of either IR or RF.
- each transmitter array can determine the location of each mobile receiver before transmission.
- for ease of tractability of the optimisation problem, illuminance sensors with no decoders are distributed across the room to ensure illuminance uniformity.

B. PROBLEM FORMULATION

The optimisation problem is formulated with the aim of minimising the luminous intensities of the transmitting arrays while fulfilling the SINR target for LITUs and taking into consideration the required minimum horizontal illuminance. For simplicity, firstly the optimisation problem is formulated with the consideration of the SINR of only LITUs while the LTUs are provided with the best case SINR levels from the system. Since the human eye perceives illuminance logarithmically, the problem may be cast as

$$(\mathbf{P1}): \underset{\mathcal{I}_{N_{l,u}}>0,\ \mathcal{I}_{N_{j,u}}\geq 0}{\texttt{minimise}} \quad \texttt{max}_{\mathsf{s}}|\log\mathcal{E}_{\mathsf{s}}^{\mathsf{tx}} - \log\mathcal{E}_{\mathsf{r}_u}|, \tag{20a}$$

$$\texttt{subject to} \quad \mathcal{I}_{N_{l,u}} \leq \mathcal{I}_{N_{l,u}}^{\mathsf{csk}}, \quad \forall l \in \mathcal{L}, \tag{20b}$$

$$\mathcal{I}_{N_{j,u}} \leq \mathcal{I}_{N_{j,u}}^{\max}, \quad \forall j \in \mathcal{L}\setminus\{l\}, \tag{20c}$$

$$\mathcal{E}_{\mathsf{s}}^{\mathsf{tx}} \geq \mathcal{E}_{\mathsf{r}_u}, \quad \forall u \in \mathcal{U}_g, \tag{20d}$$

$$\mathsf{SINR}_u \geq \gamma_u, \quad \forall u \in \mathcal{U}_g, \tag{20e}$$

where $\mathcal{I}_{N_{l,u}}^{\mathsf{csk}}$ represents the CSK modulated intensities of the transmitting array and γ_u is the LITU's SINR target.

The formulated optimisation problem is a non-convex mixed-integer non-linear programming problem. **P1** becomes intricate with an increasing number users, especially when they are moving around the room [24]. As different symbols are transmitted and the coordinates of the user's location change, the SINR level changes and the optimisation problem will have to be repeated with every change. To reduce the complexity of solving **P1** due to the aforementioned changes, the problem is solved in two parts following a pragmatic approach.

To simplify the complexity of **P1**, the proposed system model firstly re-configures the CSK-OSM scheme to re-assign the transmitting LED array based on the distance from the centre of the transmitter to the centre of the receiver. If the selected LED array is furthest from the user, the selected LED array is re-assigned to the LED array closest to the user.

Secondly, it is noted that the objective function presented in (20a) is non-convex and this makes it difficult to solve it efficiently. Nonetheless, this problem can easily be transformed into its convex equivalent based on the properties of logarithmic functions. To describe the transformation procedure, let $\texttt{max}_{\mathsf{s}}|\log\left(\mathcal{E}_{\mathsf{s}}^{\mathsf{tx}}/\mathcal{E}_{\mathsf{r}_u}\right)|$ be represented by $\texttt{max}|\log(A/B)|$, then, it follows that

$$\texttt{max}|\log(A/B)| = \begin{cases} \log(A/B), & A/B \geq 1 \\ -\log(B/A), & A/B \leq 1, \end{cases}$$

$$= \begin{cases} \arg\max\left(|\log\left(A/B\right)|\right), & A/B \geq 1 \\ \arg\max\left(|\log\left(B/A\right)|\right), & A/B \leq 1, \end{cases}$$
$$= \begin{cases} \arg\max\left(\log\left(A/B\right)\right), & A/B \geq 1 \\ \arg\max\left(\log\left(B/A\right)\right), & A/B \leq 1. \end{cases} \tag{21}$$

Based on equation 21, the objective function can be now be turned into a convex form and hence re-formulate **P1** for determination of a global solution. Hence the problem **P1** in equation 20 can now be cast as

$$(\mathbf{P2}): \underset{\mathcal{I}_{N_{l,u}}>0,\, \mathcal{I}_{N_{j,u}}\geq 0}{\texttt{minimise}} \quad \max_{\mathbf{s}} f\left(\mathcal{E}_{\mathbf{s}}^{\mathbf{tx}}/\mathcal{E}_{\mathbf{r}_u}\right), \tag{22a}$$

$$\texttt{subject to} \quad \mathcal{I}_{N_{l,u}} \leq \mathcal{I}_{N_{l,u}}^{\mathbf{csk}}, \quad \forall l \in \mathcal{L}, \tag{22b}$$
$$\mathcal{I}_{N_{j,u}} \leq \mathcal{I}_{N_{j,u}}^{\max}, \quad \forall j \in \mathcal{L}\backslash\{l\}, \tag{22c}$$
$$\mathcal{E}_{\mathbf{s}}^{\mathbf{tx}} \geq \mathcal{E}_{\mathbf{r}_u}, \quad \forall u \in \mathcal{U}_g, \tag{22d}$$
$$\mathbf{SINR}_u \geq \gamma_u, \quad \forall u \in \mathcal{U}_g, \tag{22e}$$

where $f(x) = \max\{x, 1/x\}$. It is now noted that the objective function $f(x)$ is nonlinear, non-differentiable, and convex due to monotonical increase of a logarithmic function. It is also worth noting that equation 22e is non-convex neither is it concave. For problem **P2** to be solved efficiently by the available convex optimisation techniques, the constraint stated in equation 22e should be converted into a convex function. One way to achieve convexity of equation 22e is to firstly re-write the constraint as

$$\left(\mathbf{h}_{l,u}^{\mathsf{T}}\mathbf{p}_l\right)^2 \geq \gamma_u \sum_{j\in\mathcal{L}\backslash\{l\}} \left(\mathbf{h}_{j,u}^{\mathsf{T}}\mathbf{p}_j\right)^2 + \sigma_u^2, \tag{23}$$

it then follows that, taking the square root on both sides, makes the constraint a convex second order cone constraint denoted by [25]

$$\mathbf{h}_{l,u}^{\mathsf{T}}\mathbf{p}_l \geq \sqrt{\gamma_u \sum_{j\in\mathcal{L}\backslash\{l\}} \left(\mathbf{h}_{j,u}^{\mathsf{T}}\mathbf{p}_j\right)^2 + \sigma_u^2}. \tag{24}$$

Now problem **P2** can be efficiently solved, it is however worth noting that, this optimisation problem may highly likely not satisfy the solution with equality based on the fact that this work's attempt is to satisfy two objectives, being the light intensity and the SINR target. For instance, in the event that the SINR target threshold is low, the target will be satisfied with a high SINR as compared to a higher SINR target threshold, which may likely not be satisfied due to elevated interference from the non-transmitting LED arrays. To maintain the desired illuminance during any symbol transmission while satisfying the user SINR target, Algorithm 1 is proposed.

The algorithm requires four (4) main inputs which are; maximum array intensities for all of the available light sources (LED arrays), the target SINR level for LITUs, the user required illuminance level as well as the symbols to be transmitted. The initialisation step sets the intensities of all

Algorithm 1: Algorithm for Optimal Illuminance and Symbol Transmission Under Illuminance and **LITUs' SINR** Constraints

Input: $\mathcal{I}_{N_{l,u}}^{\max}, \forall l \in \mathcal{L}, \gamma_u, \mathcal{E}_{\mathbf{r}}, \mathbf{s}_l$
Initialisation: Set $0 \leq \mathcal{I}_{N_{l,u}} \leq \mathcal{I}_{N_{l,u}}^{\max}, \forall l \in \mathcal{L}$
Result: Maintain $\mathcal{E}_{\mathbf{r}}$ and ensure γ_u

1 Set $\mathcal{E}_{\mathbf{r}}$ using (18) ; ▷ Required illuminance without transmission
2 Compute $\mathcal{E}_{\mathbf{s}}^{\max}$ using (18) ; ▷ Maximum illuminance without transmission
3 **for** $l = 1$ **to** $\mathcal{L}$ **do**
4 **for** $u = 1$ **to** $\mathcal{U}$ **do**
5 Compute $d_{l,u}$; ▷ Distance between LED array l and user u
6 Append $d_{l,u}$ to an array ;
7 **for** $u = 1$ **to** $\mathcal{U}_g$ **do**
8 Extract $d_{l,u}$ from an array in step 6 ; ▷ For **LITUs**
9 **if** $d_{l,u}$ *is the shortest to the* **LITU** **then**
10 Set l as the transmitting LED array;
11 **else**
12 Re-assign l to the LED array with the shortest distance to the **LITU**.
13 Solve **(P2)** with the constraint in (24);
14 Update $\mathcal{I}_{N_{l,u}} = \mathbf{s}_l\mathcal{I}_{N_{l,u}}^{*}$; ▷ Optimal intensity for the transmitting array
15 Set $\mathcal{I}_{N_{j,u}}^{*}, \forall j \in \mathcal{L}\backslash\{l\}$; ▷ Optimal intensities for non-transmitting arrays
16 Compute $\mathcal{E}_{\mathbf{s}}^{\mathbf{tx}*}$ using (18) ; ▷ Optimal illuminance during transmission
17 Update $\mathcal{E}_{\mathbf{r}} = \mathcal{E}_{\mathbf{s}}^{\mathbf{tx}*}$
18 **repeat**
19 Step 3
20 **until** *All symbols are transmitted*;

the LED arrays to a certain level within the acceptable indoor illuminance level. The purpose of the algorithm is to maintain the standard illuminance while ensuring that the target SINR for LITUs is met. The first step of the proposed algorithm is to set the user required illuminance before transmission of any symbol. The second step calculates the maximum illuminance that is offered by all of the LED arrays while steps 3 to 6 computes the distances between the transmitting array and the users on the receiving plane. Steps 7 to 12 of the algorithm are concerned with the selection of the transmitting LED array based on the distance between the transmitter and the receiver. If the transmitting array is closest to the receiver, the said transmitting array is used for transmission, if otherwise the transmitting LED array is re-assigned. Step 13 of Algorithm 1 is merely for solving the optimisation problem based on the stipulated constraints in order to determine the optimal LED array intensities for the required illuminance without degradation of the LITUs' SINR target. In step 14, using the optimal intensity for the transmitting array, the

TABLE 1. LED and PD simulation parameters.

	LED Chip		
Parameter	Red	Green	Blue
Peak wavelength (nm)	620	520	450
Luminous flux (lm)	140.60	230.20	60.20
Forward voltage (V)	2.30	3.70	3.50
Forward current (mA)	700	700	700
Semi-angle ($^\circ$)	60	60	60
	PD Chip		
Parameter	Red	Green	Blue
Responsivity (A/W)	0.6	0.6	0.6
Refractive index	1.5	1.5	1.5
FOV ($^\circ$)	60	60	60
Active area (cm^2)	3	3	3
Optical gain	1	1	1

algorithm alters the intensity of the transmitting array while in step 15, the intensities of the non-transmitting arrays are altered with the optimal intensities as obtained from step 13. Step 16 basically computes the optimal illuminance and subsequently in step 17, the proposed algorithm alters the required illuminance by replacing it with the optimal illuminance. Finally steps 18 through 20 are for repeating the prior steps until all of the symbols have been transmitted.

IV. SIMULATIONS

All computations for producing the simulation plots presented herein were carried out using Python 3.8.5 and CVXPY 1.0.31 [26], [27].

A. SETUP AND SIMULATION PARAMETERS

To analyse the performance of the system, computer simulations based on different configurations were carried out as described in this subsection. Transmitters are mounted to flush with the surface of the ceiling of a general indoor working space, measuring 5 m × 5 m × 3 m. The receiving plane is 1 m above the floor and the receivers are positioned facing the ceiling. There are four light fixtures which are each made up of an array of twenty (4 × 5) RGB LEDs. With reference to Figure 4, the centre of the room, on the *xy*-plane (receiving plane), is defined by coordinate (0, 0). The illuminating fixtures are positioned at (1.25, 1.25), (−1.25, 1.25), (1.25, −1.25) and (−1.25, −1.25). Each user is equipped with a receiver made up three PDs preceded by either a red, green or blue optical filter with an optical gain of unity. A selected set of parameters of the non-imaging PD and the RGB LED used for simulations are tabulated in Table 1. The LED spectra of the RGB chips making up the transmitters is shown in Figure 5(a). Figure 5(b)shows typical transmittance curves for the RGB optical filters.

B. NUMERICAL RESULTS

According to the International Organisation for Standardisation (ISO), the illuminance level of an indoor space should be from 300 lux to 1500 lux, depending on the tasks being

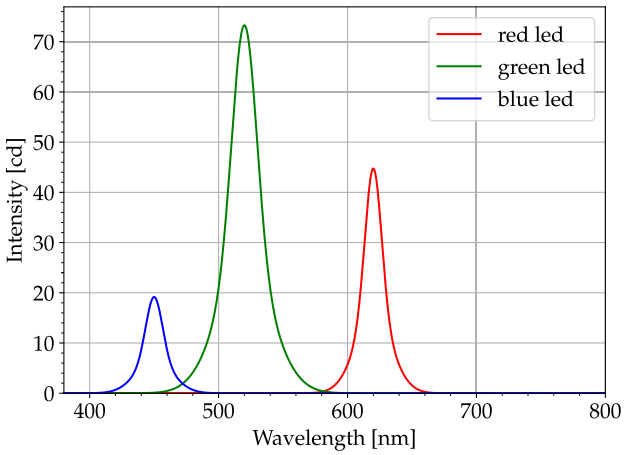

(a) LED chip spectra.

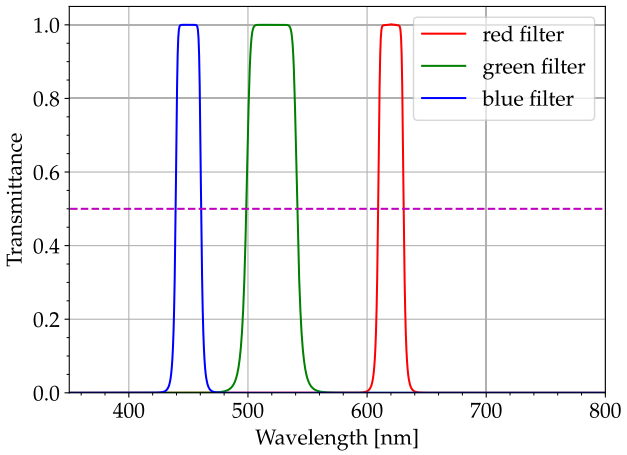

(b) Filter transmittance.

FIGURE 5. RGB LED spectra and optical filter transmittance curves.

carried out [23]. Using the parameters in Table 1, the illuminance patterns as well as the plots of the received optical power on the *xy*-plane at different points of the room for various LED array configurations are shown in Figure 6. Figure 6(a) depicts the illuminance patterns for one array located at the centre of the room, Figure 6(b) depicts the illuminance patterns for one array located at the corner of the room, Figure 6(c) depicts the illuminance patterns for two arrays located at the opposite corners of the room whereas Figure 6(d) show the illuminance pattern for four arrays located at the corners of the room. Figure 6(e) shows the plots of the received power across the room under different array configurations. As expected, configurations where a single LED array is used, low levels of illuminance are experienced, hence low optical power levels at the receiver whereas the use of numerous arrays yield higher levels of illuminance, resulting in increased optical power as seen in Figure 6(d) and Figure 6(e). Adequate and uniform levels of illuminance are in accordance with ISO standards for configurations of at least two LED arrays.

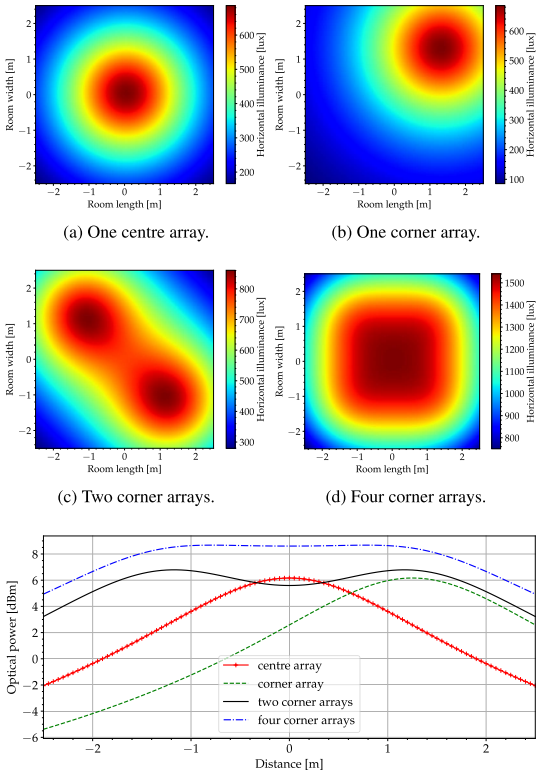

(a) One centre array. (b) One corner array.

(c) Two corner arrays. (d) Four corner arrays.

(e) Optical power contributed by different arrays at various locations.

FIGURE 6. Illuminance levels and power distribution of various array configurations without symbol transmission.

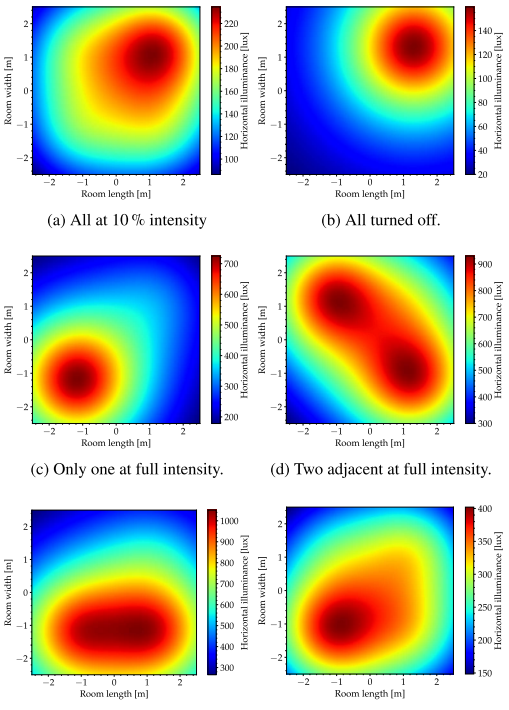

(a) All at 10 % intensity (b) All turned off.

(c) Only one at full intensity. (d) Two adjacent at full intensity.

(e) Two opposite at full intensity. (f) All at varying intensities.

FIGURE 7. Heat-maps of the illuminance with varying intensities of the non-transmitting arrays during one symbol transmission using 8CSK-OSM.

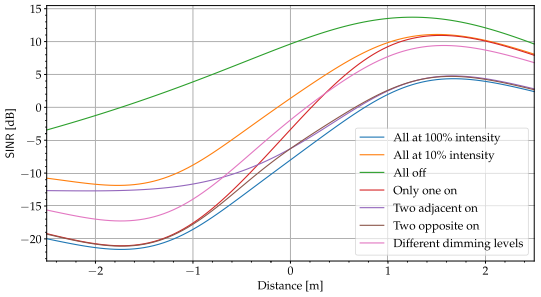

(a) SINR level variations for one symbol under varying intensities.

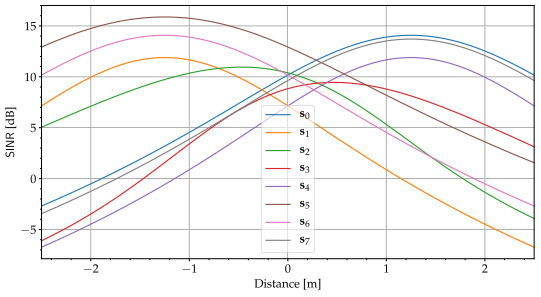

(b) SINR level variations for different symbols with all non-transmitting arrays turned off.

FIGURE 8. SINR plots across the room with varying intensities of the non-transmitting arrays during one symbol transmission using 8CSK-OSM.

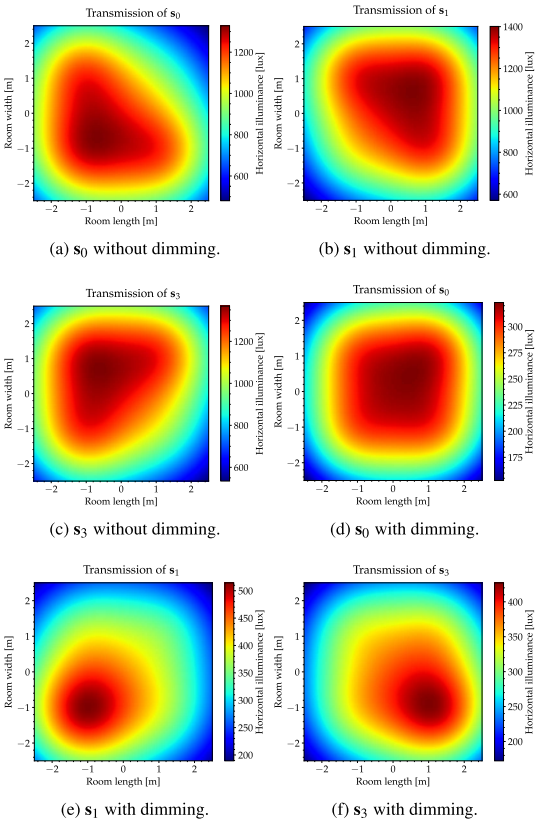

(a) $\mathbf{s}_0$ without dimming. (b) $\mathbf{s}_1$ without dimming.

(c) $\mathbf{s}_3$ without dimming. (d) $\mathbf{s}_0$ with dimming.

(e) $\mathbf{s}_1$ with dimming. (f) $\mathbf{s}_3$ with dimming.

FIGURE 9. Heat-maps of the illuminance across the room without and with dimming of the non-transmitting arrays during the transmission of different symbols using 8CSK-OSM.

Figure 7 shows the heat-maps depicting indoor illuminance levels during signal transmission under distinct intensities of the non-transmitting arrays. It is observed in Figure 7(a) to Figure 7(f) that the illuminance distribution depicted in Figure 6(d) is altered differently when the intensity combinations differ, subsequently affecting the SINR (see Figure 8(a)).

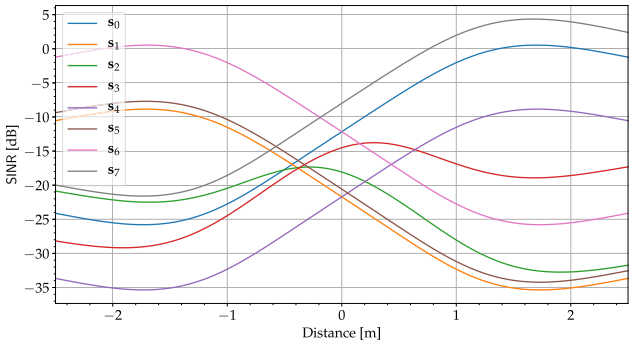

(a) SINR level variations without dimming.

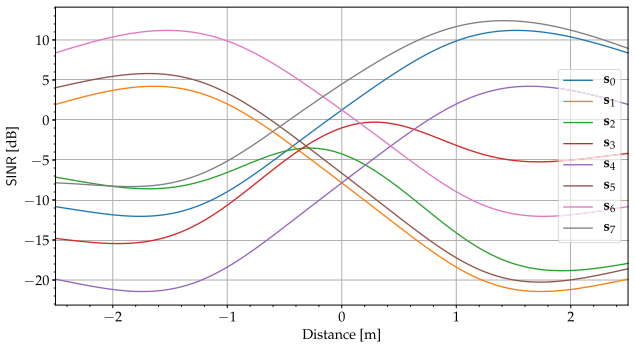

(b) SINR level variations with dimming.

FIGURE 10. SINR plots across the room without and with dimming of the non-transmitting arrays during the transmission of different symbols using 8CSK-OSM.

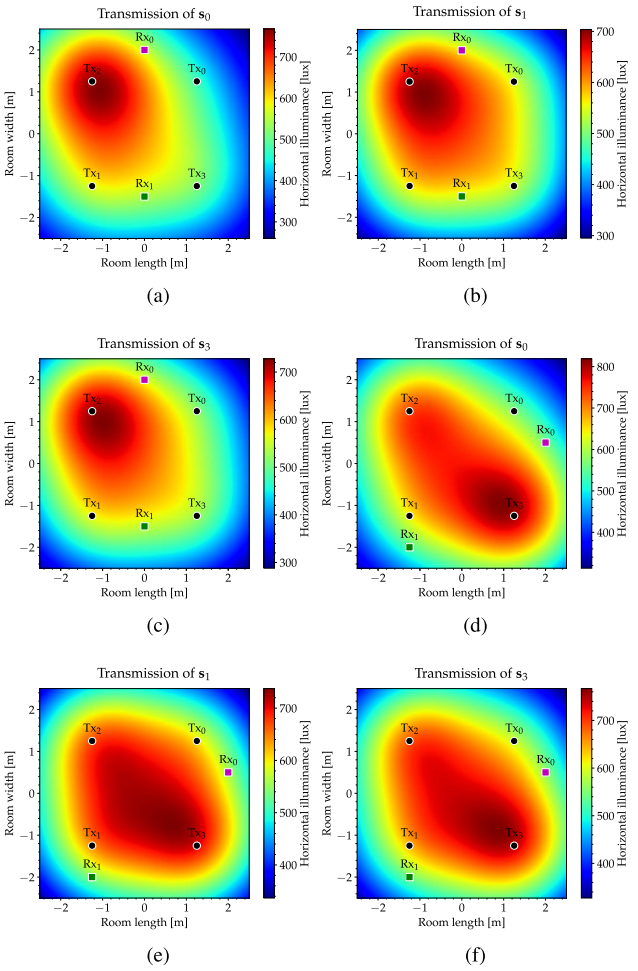

FIGURE 11. Heat-maps of the optimised illuminance offering the required illuminance of 550 lux after transmitter re-assignment but without the SINR constraint for different configurations during transmission of different symbols using 8CSK-OSM with receivers at different positions.

With reference to Figure 6(b) and Figure 7(b), illuminance levels are drastically reduced when non-transmitting arrays are off. The depictions in Figure 7, clearly show that different settings for intensity levels of the transmitting and non-transmitting arrays may lead to some challenges in relation to the minimum illuminance and signal transmission. These challenges, among others, include; high energy consumption, under utilisation of resources, high levels of interference leading to poor QoS and visual disturbance during transmission owing to non-uniform levels of illuminance. The proposed system adapts the configuration in Figure 6(d) and the intensities of the non-transmitting arrays are not equally dimmed or brightened during transmission.

The illuminance distribution patterns during symbol transmission without dimming of the non-transmitting arrays are shown in Figures 9(a) to 9(c). During the transmission of $\mathbf{s}_0$, as seen in Figure 9(a), the illuminance levels are higher for the working areas under non-transmitting arrays while there is very little illuminance for areas under the transmitting array, which is located at $(1.25, 1.25)$. The above mentioned phenomenon is perpetual during the transmission of all subsequent symbols, as depicted in Figure 9(b) for $\mathbf{s}_1$ and Figure 9(c) for $\mathbf{s}_3$ using the transmitters located at $(-1.25, -1.25)$ and $(1.25, -1.25)$, respectively. Although, illuminance levels are within the standardised levels during symbol transmission, it will be very difficult if not infeasible for the receiver to decode the transmitted symbols due to high interference levels. It is demonstrated in Figure 10(a) that, the SINR for all symbols is very low compared to Figure 8(b) where all non-transmitting arrays are turned off.

The illuminance patterns during the transmission of the same symbols as in Figures 9(a) to 9(c) when the non-transmitting LED arrays are providing only 20% of their total intensities are shown in Figures 9(d) to 9(f). Comparing Figure 10(a) and Figure 10(b), it shows that SINR improves significantly when non-transmitting arrays are dimmed. Nonetheless, this may drastically decrease the illuminance levels to below the required values at other room locations. This is observed from Figure 9(d) to Figure 9(f), where the illuminance levels at the furthest point from the transmitter are at most 200 lx during symbol transmission.

With the aid of the proposed algorithm, the sub-optimal illuminance heat-maps and the resultant SINR levels are depicted in Figures 11 to 13. The simulations that yield sub-optimal results were initially done with only the consideration of illuminance without the SINR constraint. The

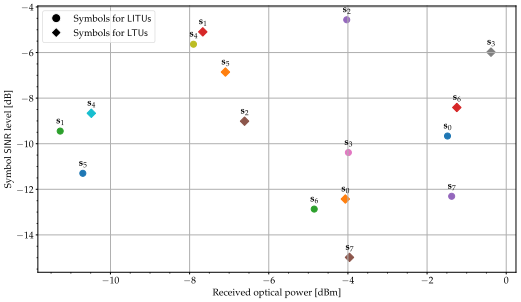

(a) SINR levels against received power for each symbol before transmitter re-assignment.

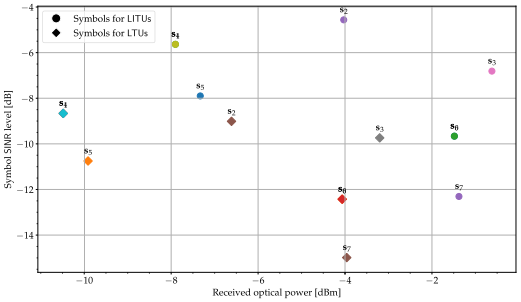

(b) SINR levels against received power for each symbol after transmitter re-assignment.

FIGURE 12. SINR levels without the SINR constraint for configuration one during transmission of different symbols using 8CSK-OSM with receivers at $(0, 2)$ (LITU location) and at $(0, -1.5)$ (LTU location).

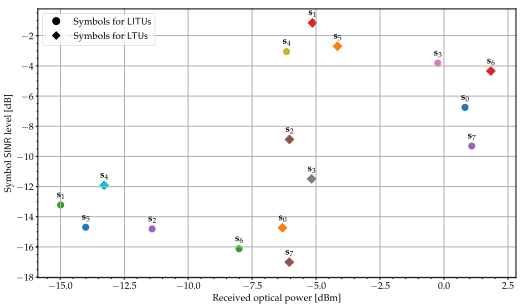

(a) SINR levels against received power for each symbol before transmitter re-assignment.

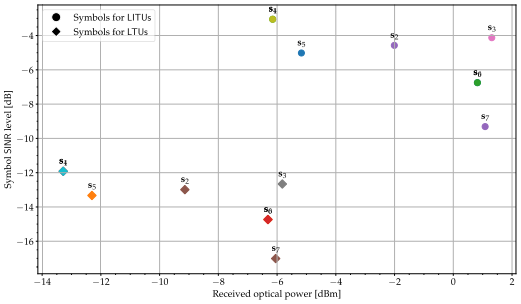

(b) SINR levels against received power for each symbol after transmitter re-assignment.

FIGURE 13. SINR levels without the SINR constraint for configuration two during transmission of different symbols using 8CSK-OSM with receivers at $(2, 0.5)$ (LITU location) and at $(-1.25, -2)$ (LTU location).

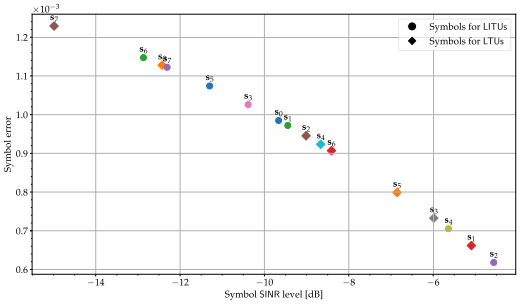

(a) Symbol error against SINR levels for each symbol before transmitter re-assignment.

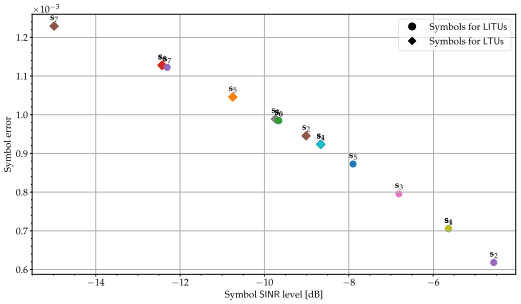

(b) Symbol error against SINR levels for each symbol after transmitter re-assignment.

FIGURE 14. Symbol error without the SINR constraint for configuration one during transmission of different symbols using 8CSK-OSM with receivers at $(0, 2)$ (LITU location) and at $(0, -1.5)$ (LTU location).

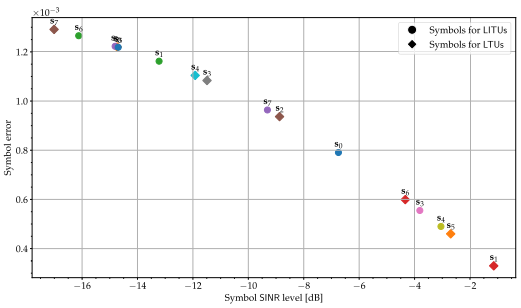

(a) Symbol error against SINR levels for each symbol before transmitter re-assignment.

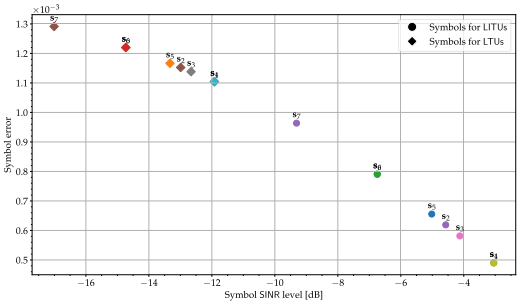

(b) Symbol error against SINR levels for each symbol after transmitter re-assignment.

FIGURE 15. Symbol error without the SINR constraint for configuration two during transmission of different symbols using 8CSK-OSM with receivers at $(2, 0.5)$ (LITU location) and at $(-1.25, -2)$ (LTU location).

optimal illuminance heat-maps and the resultant SINR levels are depicted in Figures 16 to 18. For simulations that yield the optimal results, they were carried out with the consideration of both transmitter re-assignment and the SINR constraint. In all of these maps and plots, the LITU is considered to be placed at Rx_0 while the LTU is considered to be placed

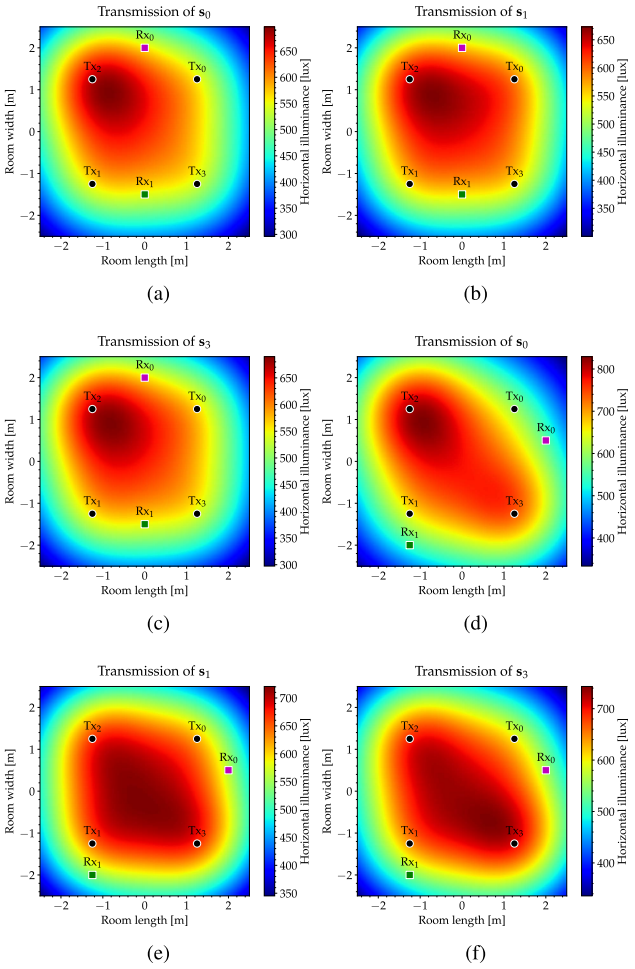

FIGURE 16. **Heat-maps of the optimised illuminance offering the required illuminance of** $550\,\text{lux}$ **and meeting the SINR level target of** $-10\,\text{dB}$ **for different configurations during transmission of different symbols using 8CSK-OSM with receivers at different positions.**

at Rx_1. Comparing Figures Figures 9(a) to 9(c) with all of the sub-figures in Figure 11, it is clear that when considering only the illumination constraint after transmitter re-assignment, the proposed algorithm is capable of satisfying the required illuminance levels (in this case, the required illuminace was set to 550 lux) at different user locations with no need to perform manual dimming. However, it is worth noting that the algorithm provides the required illuminance to the LTU mostly from the non-transmitting arrays. This means that there is a high likelihood of very poor SINR levels for latency tolerant users. This is the motivating factor for the introduction of part two of the formulated problem, however, the solution to reduce the impacts of the the said interference is not considered in this work and it forms part of the future work to be carried out. For a possible solution to the aforementioned problem, the reader is directed to the work in [28], which deals with mixed-QoS SINR balancing between LITUs and LTUs. Adaptation of the work in [28] as the solution for part two of the problem may result in the capability of providing fairness for all types of network users.

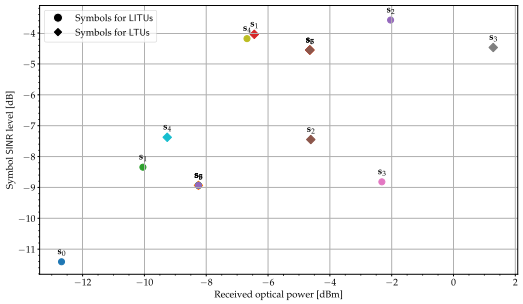

(a) SINR levels against received power for each symbol before transmitter re-assignment.

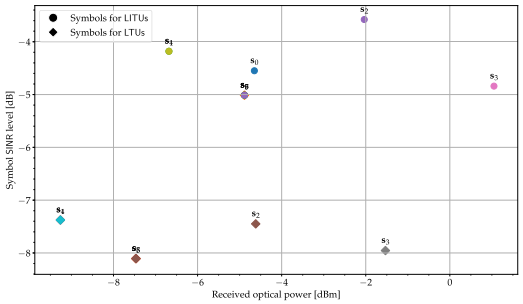

(b) SINR levels against received power for each symbol after transmitter re-assignment

FIGURE 17. **SINR levels with the SINR constraint for configuration one during transmission of different symbols using 8CSK-OSM with receivers at** $(0, 2)$ **(LITU location) and** $(0, -1.5)$ **(LTU location).**

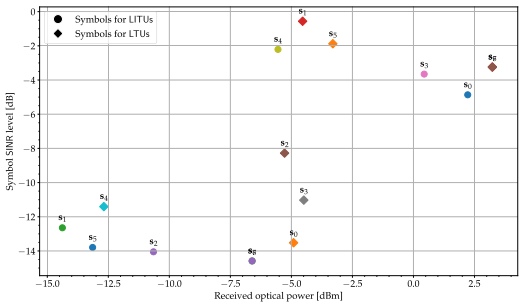

(a) SINR levels against received power for each symbol before transmitter re-assignment.

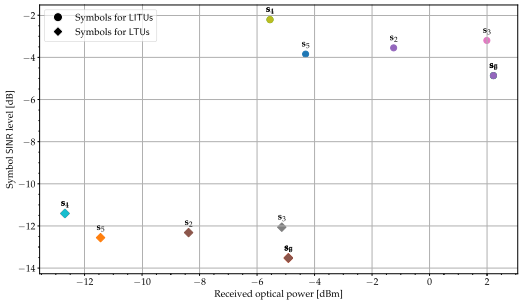

(b) SINR levels against received power for each symbol after transmitter re-assignment.

FIGURE 18. **SINR levels with the SINR constraint for configuration two during transmission of different symbols using 8CSK-OSM with receivers at** $(2, 0.5)$ **(LITU location) and at** $(-1.25, -2)$ **(LTU location).**

Figure 12 shows the SINR levels per symbol with and without transmitter re-assignment for different user configurations during symbol transmission, respectively. It should

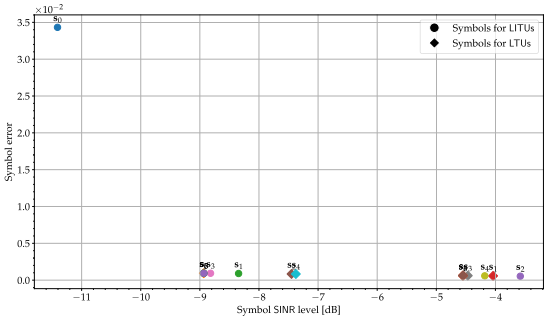

(a) Symbol error against SINR levels for each symbol before transmitter re-assignment.

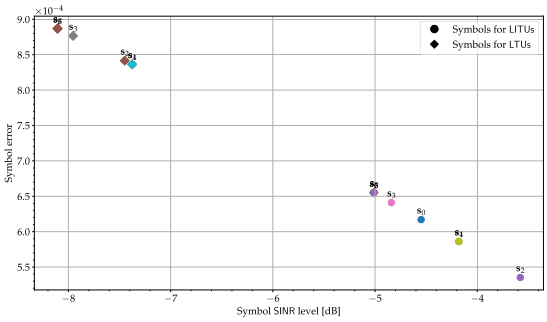

(b) Symbol error against SINR levels for each symbol after transmitter re-assignment

FIGURE 19. Symbol error with the SINR constraint for configuration one during transmission of different symbols using 8CSK-OSM with receivers at $(0, 2)$ (LITU location) and $(0, -1.5)$ (LTU location).

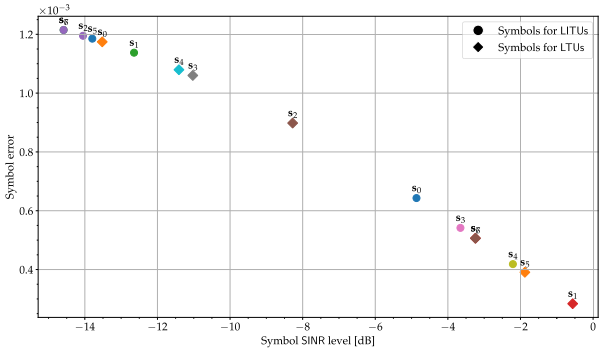

(a) Symbol error against SINR levels for each symbol before transmitter re-assignment.

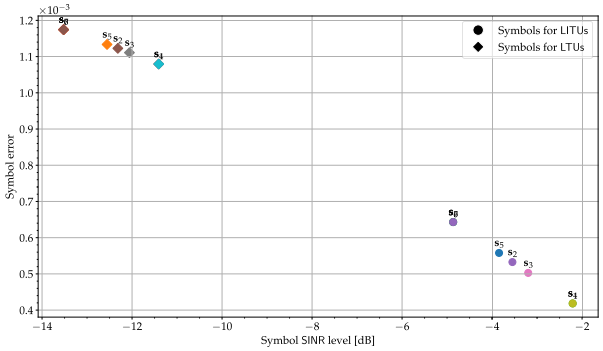

(b) Symbol error against SINR levels for each symbol after transmitter re-assignment.

FIGURE 20. Symbol error with the SINR constraint for configuration two during transmission of different symbols using 8CSK-OSM with receivers at $(2, 0.5)$ (LITU location) and at $(-1.25, -2)$ (LTU location).

be noted that some symbols are plotted on top of each other and this is attributed to the fact that, some symbols may have the same amount of power due to the nature of CSK modulation colour bands. From these plots, it suggests that the target SINR should be bounded to the maximum and minimum system values due to the varying SINR levels of the individual symbols. Moreover, the satisfaction of the SINR target largely depends on the location of the user, therefore user stations may need to be pre-defined in a practical real-time application. For mobile users, the mobile range needs to be restricted to the locality of the transmitting LED array during the transmission of a symbol.

It is observed in Figures 16(a) to 16(f), by way of comparison with Figures Figures 11(a) to 11(f) that the consideration of the SINR constraint does not affect the illuminance levels in an undesirable manner because the desired illuminance level is met in all cases. On the other hand, the simulations in Figures 17 and 18 shows that there is power reduction for all of the transmitted symbols while satisfying the SINR target, which was set to -10 dB for this simulation. However, some of CSK symbols may result in an infeasible solution in the event that the desired illuminance is very high and the transmitting power is very low. This is likely to occur during the transmission of symbols with very low optical power due to the principle of CSK modulation technique, which reduces the optical intensity of the RGB chips.

The amount of error associated with the decoded symbols is shown in Figures 14, 15, 19 and 20. It is observed in all of these figures that the magnitude of error of the decoded symbols is in the order of 10^{-2} and 10^{-4}. As expected, the symbol error for the LTUs is higher than that of the LITUs. Moreover, the transmitter re-assignment as well as the consideration of the SINR constraint significantly reduces the amount of error of the decoded symbols.

The minimum and average data rate for the types of network users are depicted in Figure 21. With reference to Figures 16 and 21, it is observed that with an increase in the number of LITU or LTU, the data rates significantly decreases due to the amount of interference from the non-transmitting arrays as they compensate for illuminance. Moreover, from Figure 21, it is evident that lower modulation orders are more robust to noise whereas higher order modulation orders are not as robust in the presence of noise despite them offering high data rate. However, with the obtained SINR levels shown in Figure 12(a) and Figure 12(b), the average data rate in worst case scenarios for both types of users for the defined room dimensions can be met with bounded SINR targets for LITUs. So, in general, the proposed algorithm, without the consideration of SINR balancing, is capable of providing the desired illuminance at all user positions with a satisfactory SINR level for LITUs, which is the main aim of this work.

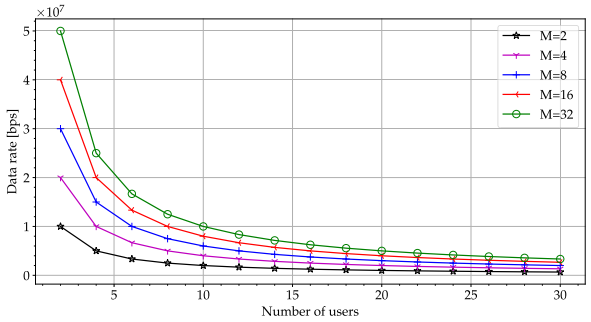

(a) Ideal data rates against the number of (LITUs) and (LTUs).

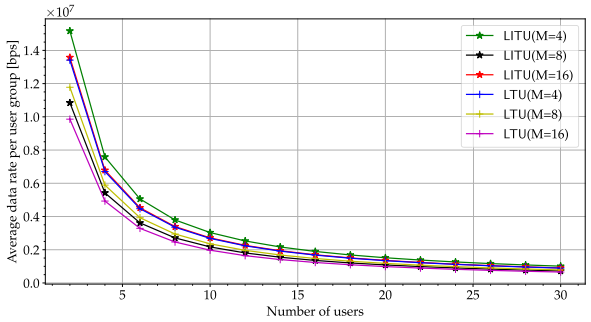

(b) Average data rates against the number of (LITUs) and (LTUs) without both transmitter re-assignment and SINR constraint.

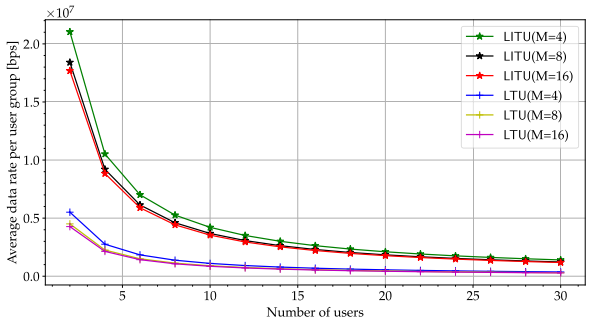

(c) Average data rates against the number of (LITUs) and (LTUs) after transmitter re-assignment and without SINR constraint.

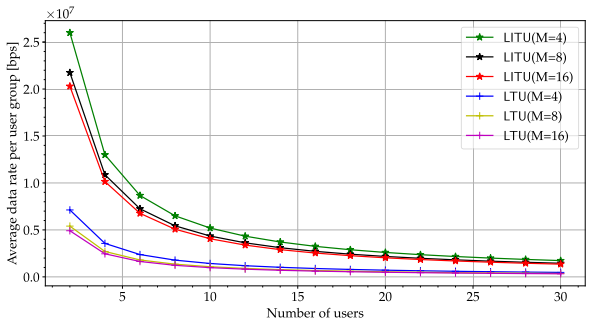

(d) Average data rates against the number of (LITUs) and (LTUs) with both transmitter re-assignment and SINR constraint.

FIGURE 21. Effects of the CSK modulation order, transmitter re-assignment and SINR constraint on the data rates for LITUs and LTUs for various CSK modulation orders.

V. CONCLUSION

In this paper, an algorithm for the optimisation of a colour-based optical spatial modulation scheme for visible light communication (VLC) was proposed. The proposed scheme is based on the joint utilisation of CSK and OSM with IM/DD. The aim was to ensure that the illuminance levels are not affected by the optical intensity variations which arise due to CSK modulation while minimising the amount of optical power used for symbol transmission without depreciation of the SINR target. In comparison to other VLC works, where the conventional spatial modulation is applied, this paper proposed a low-complexity algorithm with the consideration of heterogeneous network users with minimal error of the decoded symbols. The proposed algorithm is capable of satisfying the user's required illuminance level provided it is specified within the recommended levels as per the ISO standards. Furthermore, the algorithm can meet the SINR targets for the LITUs while minimising the optical power of the LED arrays without affecting the required illuminance level. That being said, in general terms, the proposed algorithm is capable of providing the desired illuminance at all user positions with reduced optical intensity and a satisfactory SINR level for almost all of the transmitted symbols, with the exception of the symbols that are transmitted with limited power due to CSK modulation technique. One of the shortfalls of this work is that it does not guarantee acceptable SINR levels for LTUs. Additionally, this work did not consider illumination uniformity to ensure standard illuminance levels for the entire room. In the future, the authors intend to introduce the second part of the problem to deal with mixed QoS through the adaptation of distributed algorithms used in radio frequency systems as well as the introduction of additional constraints to the optimisation problems to deal with illuminance uniformity. Lastly, the re-assignment of the transmitting LED array may lead to very poor SINR levels for the latency-tolerant network users even when the fairness approach offered by distributed algorithms is applied. Therefore, it is of significance to investigate other spatial modulation techniques such as the generalised spatial modulation.

REFERENCES

[1] S. Li, L. Wang, N. Hirosaki, and R. Xie, "Color conversion materials for high-brightness laser-driven solid-state lighting," *Laser Photon. Rev.*, vol. 12, no. 12, Dec. 2018, Art. no. 1800173.

[2] S. Bhardwaj, T. Ozcelebi, R. Verhoeven, and J. Lukkien, "Smart indoor solid state lighting based on a novel illumination model and implementation," *IEEE Trans. Consum. Electron.*, vol. 57, no. 4, pp. 1612–1621, Nov. 2011.

[3] T. M. Katona, P. M. Pattison, and S. Paolini, "Status of solid state lighting product development and future trends for general illumination," *Annu. Rev. Chem. Biomolecular Eng.*, vol. 7, no. 1, pp. 263–281, Jun. 2016.

[4] B. Janjua, H. M. Oubei, J. R. D. Retamal, T. K. Ng, C.-T. Tsai, H.-Y. Wang, Y.-C. Chi, H.-C. Kuo, G.-R. Lin, J.-H. He, and B. S. Ooi, "Going beyond 4 Gbps data rate by employing RGB laser diodes for visible light communication," *Opt. Exp.*, vol. 23, no. 14, p. 18746, Jul. 2015.

[5] R. Mesleh, R. Mehmood, H. Elgala, and H. Haas, "Indoor MIMO optical wireless communication using spatial modulation," in *Proc. IEEE Int. Conf. Commun. (ICC)*, Cape Town, South Africa, May 2010, pp. 1–5.

[6] P. M. Butala, H. Elgala, and T. D. C. Little, "Performance of optical spatial modulation and spatial multiplexing with imaging receiver," in *Proc. IEEE WCNC*, Apr. 2014, pp. 394–399.

[7] *IEEE Standard for Local and Metropolitan Area Networks—Part 15.7: Short-Range Optical Wireless Communications IEEE Standard*, Standard 802.15.7-2018, 2018.

[8] Y. Chen and M. Jiang, "Joint colour-and-spatial modulation aided visible light communication system," in *Proc. IEEE 83rd Veh. Technol. Conf. (VTC Spring)*, Nanjing, China, May 2016, pp. 1–5.

[9] M. Guo, Z. Bai, K. Pang, X. Hao, J. Tian, and K. Kwak, "Color space and multi-stream spatial modulation based indoor visible light communication," in *Proc. Int. Wireless Commun. Mobile Comput. (IWCMC)*, Jun. 2020, pp. 1091–1095.
[10] *International Commission on Illumination, Colorimetry—Part 3: CIE Tristimulus Values*, document ISO 11664-3:2012(E)/CIE S014-3/E, 2011. [Online]. Available: http://www.cie.co.at/publications/colorimetry-part-3-cie-tristimulus-values
[11] H. G. Olanrewaju, J. Thompson, and W. O. Popoola, "Performance of optical spatial modulation in indoor multipath channel," *IEEE Trans. Wireless Commun.*, vol. 17, no. 9, pp. 6042–6052, Sep. 2018.
[12] R. Mesleh, H. Elgala, and H. Haas, "Optical spatial modulation," *J. Opt. Commun. Netw.*, vol. 3, no. 3, p. 234, Mar. 2011.
[13] T. Fath and H. Haas, "Performance comparison of MIMO techniques for optical wireless communications in indoor environments," *IEEE Trans. Commun.*, vol. 61, no. 2, pp. 733–742, Feb. 2012.
[14] E. Monteiro and S. Hranilovic, "Design and implementation of color-shift keying for visible light communications," *J. Lightw. Technol.*, vol. 32, no. 10, pp. 2053–2060, May 15, 2014.
[15] J. M. Luna-Rivera, R. Perez-Jimenez, J. Rabadan-Borjes, J. Rufo-Torres, V. Guerra, and C. Suarez-Rodriguez, "Multiuser CSK scheme for indoor visible light communications," *Opt. Exp.*, vol. 22, no. 20, Oct. 2014, Art. no. 24256.
[16] F. Durukan, B. M. Guney, and A. Ozen, "Performance analysis of color shift keying systems in AWGN and color noise environment," in *Proc. 27th Signal Process. Commun. Appl. Conf. (SIU)*, Apr. 2019, pp. 1–4.
[17] Z. Ghassemlooy, W. Popoola, and S. Rajbhandari, *Optical Wireless Communications: System and Channel Modelling With MATLAB*. Boca Raton, FL, USA: CRC Press, 2013.
[18] R. Singh, T. O'Farrell, and J. P. David, "An enhanced color shift keying modulation scheme for high-speed wireless visible light communications," *J. Lightw. Technol.*, vol. 32, no. 14, pp. 2582–2592, Jun. 4, 2014.
[19] M. Abuthinien, S. Chen, A. Wolfgang, and L. Hanzo, "Joint maximum likelihood channel estimation and data detection for MIMO systems," in *Proc. IEEE Int. Conf. Commun.*, Jun. 2007, pp. 5354–5358.
[20] C. Zhu, "Hierarchical colour-shift-keying aided layered video streaming for the visible light downlink," *IEEE Access*, vol. 4, pp. 3127–3152, 2016.
[21] P. Saengudomlert, "Transmit beamforming for line-of-sight MIMO VLC with IM/DD under illumination constraints," in *Proc. 12th Int. Conf. Elect. Eng. Electron., Comput. Telecommun. Inf. Technol. (ECTI)-(CON)*, Jun. 2015, pp. 1–4.
[22] T. Komine and M. Nakagawa, "Fundamental analysis for visible-light communication system using LED lights," *IEEE Trans. Consum. Electron.*, vol. 50, no. 1, pp. 100–107, Feb. 2004.
[23] *Lighting of Work Places—Part 1: Indoor*, document ISO 8995-1:2002(en)) ISO, Tech. Rep., 2002.
[24] A. Dey, "Resource optimization in visible light communication using resource optimization in visible light communication using Internet of Things Internet of Things," Ph.D. dissertation, Dept. Elect. Comput. Eng., College Eng. Comput. Sci., Univ. Central Florida, Orlando, FL, USA, 2019.
[25] E. Björnson, M. Bengtsson, and B. Ottersten, "Optimal multiuser transmit beamforming: A difficult problem with a simple solution structure [lecture notes]," *IEEE Signal Process. Mag.*, vol. 31, no. 4, pp. 142–148, Jul. 2014.
[26] A. Agrawal, R. Verschueren, S. Diamond, and S. Boyd, "A rewriting system for convex optimization problems," *J. Control Decis.*, vol. 5, no. 1, pp. 42–60, 2018.
[27] S. Diamond and S. Boyd, "CVXPY: A Python-embedded modeling language for convex optimization," *J. Mach. Learn. Res.*, vol. 17, no. 83, pp. 1–5, Apr. 2016.
[28] B. Basutli and S. Lambotharan, "Distributed beamformer design under mixed SINR balancing and SINR-target-constraints," in *Proc. IEEE Int. Conf. Digit. Signal Process. (DSP)*, Jul. 2015, pp. 530–534.

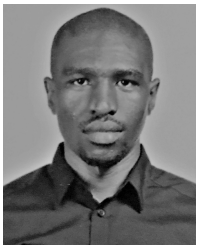

GALEFANG A. MAPUNDA received the bachelor's degree in electrical and telecommunications engineering from the Durban University of Technology (DUT), Durban, South Africa, in 2017, and the M.Eng. degree in computer and telecommunications engineering with focus on visible light communication (VLC) from the Botswana International University of Science and Technology (BIUST), Palapye, Botswana, in 2021. He was a Research Assistant at the National Astronomical Research Institute of Thailand (NARIT), from 2019 to 2021. He previously worked as an Electronic Technician at the South African Radio Observatory (SARAO), from 2014 to 2015. His research interests include wireless communications, quantum plasmonic circuits, astronomical instrumentation (both radio and optical), signals and systems, convex optimization, clinical, financial, and space engineering.

ABRAHAM SANENGA received the B.Sc. degree in electronics engineering from the University of Kwazulu Natal, in 2018. He is currently pursuing the master's degree in telecommunications and computer engineering with the Botswana International University of Science and Technology. He is also working as a Research Assistant at the National Astronomical Research Institute of Thailand. His research interest includes physical layer security in wireless communication.

BOKAMOSO BASUTLI (Senior Member, IEEE) received the Ph.D. degree in electronic, electrical, and systems engineering from Loughborough University, U.K., in 2016. His Doctoral Thesis titled "Distributed Optimization Techniques for Wireless Networks," dealt with using economics models to optimize resource allocation in wireless cellular networks. From 2008 to 2010, he was an Installation Engineer and a Lead Engineer with Singapore Technologies Electronics (Info-Software Systems), respectively. He was a Senior Telecommunications Engineer with the Civil Aviation Authority of Botswana (CAAB), from 2010 to 2012. He joined the Botswana International University of Science and Technology (BIUST), as a Founding Teaching Instructor, in 2012, where he is currently working as a Senior Lecturer with the Department of Electrical, Computer, and Telecommunications Engineering. He is also leading the Signal Processing, Networks, and Systems Research (SPNS) Group. His research interests include convex optimization, resource allocation, wireless communications, space technology, and game theory. In January 2019 and 2020, he was elected as the Vice-Chairperson and an Executive Member of the IEEE Botswana Sub-Section. He is also serving in Frontiers Editorial Board as a Review Editor on the Editorial Board for *Signal Processing for Communications* (Specialty Section of Frontiers in Signal Processing) and an Editorial Board for *IoT and Sensor Networks*. He is also a Reviewer of IEEE Communication Letters, IEEE Access, *IET Communications*, and *IET Journal of Engineering*. He is also a Professional Engineer Registered with the Engineers Registration Board (ERB), Botswana.

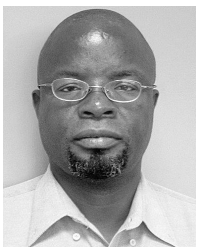

JOSEPH M. CHUMA (Member, IEEE) received the Ph.D. degree in electronic systems engineering from the University of Essex, in 2001. He was an Associate Professor with the University of Botswana and the Dean of the Faculty of Engineering and Technology. He joined the Department of Electrical, Computer and Telecommunication Engineering, Botswana International University of Science and Technology, as an Associate Professor of telecommunications engineering, in 2014, where he is currently working as the Dean of the Faculty of Engineering and Technology. He has over 24 years of experience in teaching and research, consultancy, and human resources development in telecommunication, computer, and electrical and electronics engineering, including CISCO computer networking. He has authored or coauthored three books, three book chapters, and many refereed published scholarly/scientific journal articles in the subject of telecommunications engineering. He holds three patents. He is a member of several professional bodies among which includes the IET, U.K.; and BIE, Botswana. He is a Professional Engineer Registered with the Botswana Engineers Registration Board.